Rock Mech Rock Eng (2017) 50:2235–2242
DOI 10.1007/s00603-017-1243-x

TECHNICAL NOTE

Establishing Empirical Relationships for the Effects of Water Content on the Mechanical Behavior of Gosford Sandstone

Hossein Masoumi[1] · **James Horne**[1] · **Wendy Timms**[1]

Received: 4 August 2016 / Accepted: 23 May 2017 / Published online: 31 May 2017

Keywords Gosford sandstone · Uniaxial compressive strength · Point-load index · Tensile strength · Water content

List of symbols

UCS	Uniaxial compressive strength
E	Young's modulus
PLI	Point-load index
TS	Tensile strength
ω	Water content
M_{ps}	Mass of rock sample under partially saturated condition
M_d	Mass of dry rock sample
r	Radius of the sample
H	Hydraulic diffusivity
k	Permeability
B	Skempton's coefficient
K	Bulk modulus
η	Fluid viscosity
α	Biot's coefficient
P	Maximum applied load measured during the point loading
D	Distance between two pointers (conical platens) in diametral point-load test which is also the core sample diameter
L	Length of the core sample
F	Peak load measured during the Brazilian or indirect tensile test
T	Thickness of the sample measured at the center
σ_n	Nominal strength such as UCS, E, PLI, TS
a, b and c	Material constants in Hawkins and McConnell (1992) model

✉ Hossein Masoumi
hossein.masoumi@unsw.edu.au

[1] School of Mining Engineering, UNSW Australia, Sydney, NSW 2052, Australia

1 Introduction

Mechanical properties of intact rocks, such as uniaxial compressive strength (UCS), Young's modulus (E) and tensile strength (TS), are the key factors in rock engineering and are commonly the first parameters to be characterized for any designing process. In many projects, point-load index (PLI) is measured to indirectly estimate the UCS of the intact rock. The influence of water on the mechanical behavior of rocks can be problematic for the stability of rock mass in different civil and mining structures. Many studies have attempted to address these effects experimentally and analytically (Duda and Renner 2013; Erguler and Ulusay 2009; Fischer and Paterson 1992; Hawkins and McConnell 1992; Lisabeth and Zhu 2015; Nicolas et al. 2016; Ojo and Brook 1990; Rutter 1974; Wong and Jong 2014; Zhou et al. 2016), and it has been confirmed by different researchers that an increase in water content can lead to a decrease in the strength of intact rock (Baud et al. 2000; Chenevert 1970; Lashkaripour and Passaris 1995; Li and Reddish 2004; Lia et al. 2012; Töröka and Vásárhelyib 2010; Vásárhelyia and Vánb 2006; Zhou et al. 2016).

Previous studies constrain general trends for sandstones. Hadizdeh and Law (1991) reported strength reduction of 55% in Pennant sandstone. Vásárhelyia (2005) showed a reduction in strength of 45 sandstone samples in the presence of water. Yet, Gosford sandstone (also known as Hawkesbury or Sydney sandstone) has not been specifically tested for its mechanical properties at different water

contents and under various testing conditions including uniaxial compression, point loading and indirect tension or Brazilian test. Gosford sandstone is commonly excavated in civil construction and coal mining across the Sydney Basin and is used for civil construction throughout Australia. Predictive findings regarding the mechanical properties of Gosford sandstone would therefore be beneficial to effective design and operations of many projects.

In this research, the effect of water content on the mechanical properties of Gosford sandstone is examined mainly from experimental viewpoint. It is shown that UCS, E, PLI and TS reduce with an increase in water content. An empirical model proposed by Hawkins and McConnell (1992) is then fitted to these mechanical parameters at varying water contents. Finally, it is shown that the prediction of the empirical models agree well with the experimental data.

2 Material and Testing Procedures

Gosford sandstone forms a unit within the massive (290 m thick) Triassic Hawkesbury sandstone of the Sydney Basin, New South Wales, Australia (Ord et al. 1991). In this study, a number of experiments were performed on samples of Gosford sandstone including uniaxial compressive, point-load and Brazilian tests according to International Society for Rock Mechanics (ISRM 2007). Cylindrical samples with a diameter of 42 mm were cored from blocks. The rock samples were homogenous and free of any coloring or macroscale defects. Masoumi et al. (2016b) performed X-ray diffraction analysis on the same batch of Gosford sandstone used in this study and found that it consists of 86% quartz, 7% illite, 6% kaolinite and 1% anatase. Also, Masoumi et al. (2016b) estimated the maximum grain size of this sandstone to 0.6 mm. Sufian and Russell (2013) and Roshan et al. (2016) reported a total porosity of this sandstone at about 18% based on X-ray computed tomography scans. Sufian and Russell (2013) also showed that the density distribution of the pre-existing micro-cracks within the matrix of Gosford sandstone is homogenous.

2.1 Water Saturation Technique

All samples were oven-dried for 24 h at a temperature of 105 °C to assure that they were completely dry prior to testing. The suggested method by ASTM (2010) was modified to rapidly saturate the rock samples. The core samples were soaked in de-ionized water in an acrylic chamber, and a vacuum pump was used to minimize the air inside the core. The saturation process was considered to be complete when the release of air bubbles from the cores ceased. The saturation of the core samples at lower levels was achieved by trial and error where the duration of the saturation was less than that of the full saturation. Results showed that there was an exponential increase in saturation levels up to an approximately 50%. Longer soaking time was necessary for higher saturation.

The saturation technique used in this study was similar to that employed by Zhou et al. (2016) and Yao et al. (2016) who studied the effect of water content on the mechanical properties of a fine-grained sandstone and a coal, respectively. Such a technique led to a non-uniform distribution of water inside the core samples (particularly at lower saturation levels) which was designed to replicate the natural water content condition of rock blocks in civil and open cut mining projects. The rocks at the ground surface are typically affected by seasonal rainfalls where the water soaks the rocks from the surface into the deeper layers resulting in non-uniform saturation. This condition was applied here, and all the samples were saturated heterogeneously.

The water content was calculated based on the suggested formula by ISRM (Franklin et al. 1979; ISRM 2007) which was employed by Zhou et al. (2016) and Yao et al. (2016). The change in the mass of the rock sample was used to estimate the water content of the samples at different saturation levels according to:

$$\omega = \frac{M_{ps} - M_d}{M_d} \times 100 \quad (1)$$

where ω represents the water content expressed as percentage, M_{ps} is the mass of rock sample under partially saturated condition, and M_d is the mass of dry rock sample.

2.2 Uniaxial Compressive Test

The core samples for uniaxial compressive tests were prepared with the length-to-diameter ratio of 2.5 as recommended by ISRM (2007). A total of 25 samples were tested under uniaxial compression at varying water contents (ranging from completely dry to about 7% water content) using a servo-controlled loading frame with a 150-ton maximum loading capacity. The strain rate was set at 3×10^{-5} s^{-1} to allow the samples reach failure within 5–10 min (Bieniawski and Bernede 1979; ISRM 2007). From each test, the complete stress–strain curve was recorded to determine UCS and E (Fairhurst and Hudson 1999; ISRM 2007). The uniaxial compressive tests were nominally conducted under drained condition where the samples were not jacketed. However, during the experiment some water may remain far from the pressure equilibrium at the center of the sample since the imposed strain rate may be too fast compared to the time scale of pressure diffusion. In that case, the condition might be considered undrained in the

sense that pore pressure is not constant everywhere inside the sample. In order to confirm whether the tests were under drained or undrained condition, a simple quantitative analysis is performed similar to that employed by Nicolas et al. (2016). The fluid diffusion time can be approximated according to Nicolas et al. (2016):

$$t \approx \frac{r^2}{H} \tag{2}$$

where H is the hydraulic diffusivity and r is the radius of the sample which is the minimum distance from the center of the sample to a free surface. H can be approximated using the following equation (Kumpel 1991):

$$H \approx \frac{kBK}{\eta\alpha} \tag{3}$$

where k is the permeability of the porous material, B is the Skempton's coefficient, K is the bulk modulus of the porous material, η is the viscosity of fluid, and α is the Biot's coefficient. Roshan et al. (2015) reported the permeability of Gosford sandstone used in this study at 13.4×10^{-5} m^2, η for water is about 1×10^{-3} Pa s, and K for this sandstone is 7.8 GPa according to Masoumi et al. (2016a). If B and α are assumed unity similar to Nicolas et al. (2016), then for the tested samples where $r = 21$ mm, the resulting fluid diffusion time (t) is approximately 4.2×10^{-13} s. This is a very short time compared to the testing period (between 5 and 10 min) utilized here which confirms that the experiments were conducted under drained condition.

Table 1 Uniaxial compressive strength (UCS) and Young's moduli data obtained from uniaxial compressive tests

Sample no.	Water content (%)	UCS (MPa)	Young's modulus (GPa)
UG 1	0.00	43.98	6.58
UG 2	0.00	49.23	7.36
UG 3	0.00	47.01	7.04
UG 4	0.00	46.76	7.02
UG 5	0.00	49.46	7.36
UG 6	0.00	42.05	6.15
UG 7	1.07	26.17	4.90
UG 8	1.52	23.74	5.86
UG 9	1.61	24.53	4.12
UG 10	1.65	26.04	4.66
UG 11	2.24	27.07	4.78
UG 12	2.32	26.32	4.89
UG 13	2.29	28.13	5.21
UG 14	2.42	32.35	5.85
UG 15	2.48	25.14	4.09
UG 16	3.28	23.94	4.82
UG 17	3.81	20.26	4.06
UG 18	4.27	20.82	4.12
UG 19	4.74	19.20	3.89
UG 20	6.66	14.59	3.67
UG 21	6.79	14.10	2.94
UG 22	6.83	15.04	3.13
UG 23	6.87	10.94	2.11
UG 24	6.88	13.61	2.88
UG 25	6.90	11.69	1.98

2.3 Point-Load Test

In total 44 samples were tested by point loading including 23 under axial direction and 21 under diametral orientation. The length-to-diameter ratio of the samples was one (Franklin 1985; ISRM 2007).

According to ISRM (Franklin 1985; ISRM 2007) the diametral point-load index is defined from the following equation:

$$\mathrm{PLI} = \frac{P}{D^2} \tag{4}$$

where P is the maximum applied load measured during the test and D is the distance between two pointers (conical platens) which is also the diameter of the sample. The load is applied at least 0.5 D from one end of the sample as suggested by ISRM (Franklin 1985; ISRM 2007).

For the axial test, the point-load index is calculated according to:

$$\mathrm{PLI} = \frac{P}{4LD/\pi} \tag{5}$$

where LD is the minimum cross-sectional area of a plane through the pointers and P is the applied load. In this condition, the loading is applied at the center of the end surfaces as specified by ISRM (Franklin 1985; ISRM 2007).

2.4 Indirect Tensile or Brazilian Test

For Brazilian test, ISRM (2007) has specified a length-to-diameter ratio between 0.3 and 0.6; thus, 0.5 was selected as an appropriate ratio in this study. The tensile strength (TS) is calculated using the following formula (Bieniawski and Hawkes 1978; ISRM 2007):

$$\mathrm{TS} = \frac{2F}{\pi Dt} \tag{6}$$

where F is the peak load at failure, D is the diameter, and t is the thickness of the sample measured at the center. A total of 25 tests were conducted under indirect tensile condition as specified by ISRM (2007).

Table 2 Point-load index (PLI) data obtained from point-load tests

Sample no.	Water content (%)	PLI (MPa)
PG 1	0.00	3.65
PG 2	0.00	3.85
PG 3	0.00	3.78
PG 4	0.00	3.68
PG 5	0.00	3.69
PG 6	2.23	2.48
PG 7	2.42	2.18
PG 8	2.40	2.30
PG 9	2.47	2.36
PG 10	2.56	2.23
PG 11	4.28	1.85
PG 12	4.35	1.82
PG 13	4.49	1.70
PG 14	4.56	1.71
PG 15	4.76	1.84
PG 16	6.20	1.20
PG 17	6.38	1.47
PG 18	6.50	1.22
PG 19	6.54	1.18
PG 20	6.59	1.14
PG 21	7.43	1.10

Table 3 Tensile strength (TS) data obtained from Brazilian tests

Sample no.	Water content (%)	TS (MPa)
BG 1	0.00	4.98
BG 2	0.00	4.38
BG 3	0.00	4.40
BG 4	0.00	3.78
BG 5	0.00	4.27
BG 6	1.90	2.80
BG 7	1.90	2.30
BG 8	1.90	2.96
BG 9	1.90	3.52
BG 10	1.90	3.27
BG 11	2.85	2.12
BG 12	3.04	1.85
BG 13	3.02	2.15
BG 14	3.19	2.11
BG 15	3.17	2.19
BG 16	4.25	2.45
BG 17	4.75	1.71
BG 18	4.72	2.06
BG 19	4.88	1.90
BG 20	5.03	1.99
BG 21	6.73	1.92
BG 22	6.98	1.82
BG 23	6.91	1.84
BG 24	7.04	2.02
BG 25	7.38	1.88

3 Experimental Results and Comparison with Previous Work

To estimate the variation of the mechanical parameters (UCS, E, PLI and TS) with water content, the model developed by Hawkins and McConnell (1992) was employed which utilizes the simple relationship as follows:

$$\sigma_n = ae^{-b\omega} + c \tag{7}$$

where ω was already defined in Eq. (1), σ_n is the nominal strength (e.g., UCS, PLI, TS or E), and a, b and c are material constants.

All the tested mechanical parameters decrease with an increase in water content (the detailed results are given in Tables 1, 2 and 3). Also the resulting parameters from fitting Eq. (7) to the experimental data are presented in Table 4 at 99 and 95% confidence intervals. The experimental observations are reasonably fit by Eq. (7) for all data including UCS, E, PLI and TS (see Figs. 1, 2, 3 and 4). The validity range of the fitting parameters was estimated, and the upper and lower limits are also plotted in Figs. 1, 2, 3 and 4.

The estimation of constants a and b was sufficient to attain the best fits of Eq. (7) to the mechanical parameters of Gosford sandstone at varying water contents. In other words, a good fit was obtained without the constant c, resulting in a simpler and more versatile approach to applying the Hawkins and McConnell (1992) empirical model.

An interesting finding from the axial point-load tests was associated with the invalid failure patterns observed for all samples saturated at different water contents. This is a novel observation which has not been reported previously. It is hypothesized that while the saturation progresses from the end surface of the sample inward, the sample edges become the weakest points due to the presence of water (Baud et al. 2000) resulted from heterogeneous saturation. Thus, when the stress increases, cracking propagates toward this weak zone rather than the dry zone at the center of the sample. In addition, the end surfaces flaws of the rock samples which are induced during the sample preparation process can contribute to this behavior as reported by Masoumi et al. (2016b). Figure 5 illustrates the failed samples under axial loading where a number of partially saturated samples resulted in invalid failures.

Table 4 Estimated Hawkins and McConnell (1992) model constants for different data sets

Data sets	Resulting model constants			99% Confidence intervals		95% Confidence intervals	
	a (MPa)	*b*	*c*	*a* (MPa)	*b*	*a* (MPa)	*b*
UCS	43.63	0.20	0	±4.34	±0.05	±3.20	±0.04
E	6690	0.13	0	±600	±0.04	±440	±0.03
PLI	3.69	0.17	0	±0.14	±0.02	±0.11	±0.01
TS	4.12	0.15	0	±0.51	±0.05	±0.37	±0.03

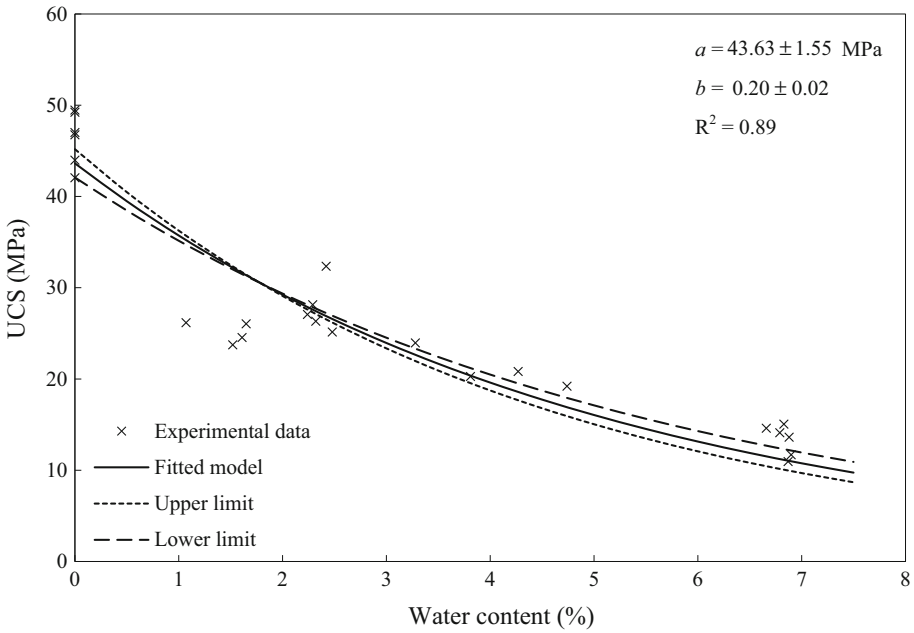

Fig. 1 Uniaxial compressive strength results obtained from different water contents having Hawkins and McConnell (1992) empirical model fitted to the data along with the validity range of the fitting parameters

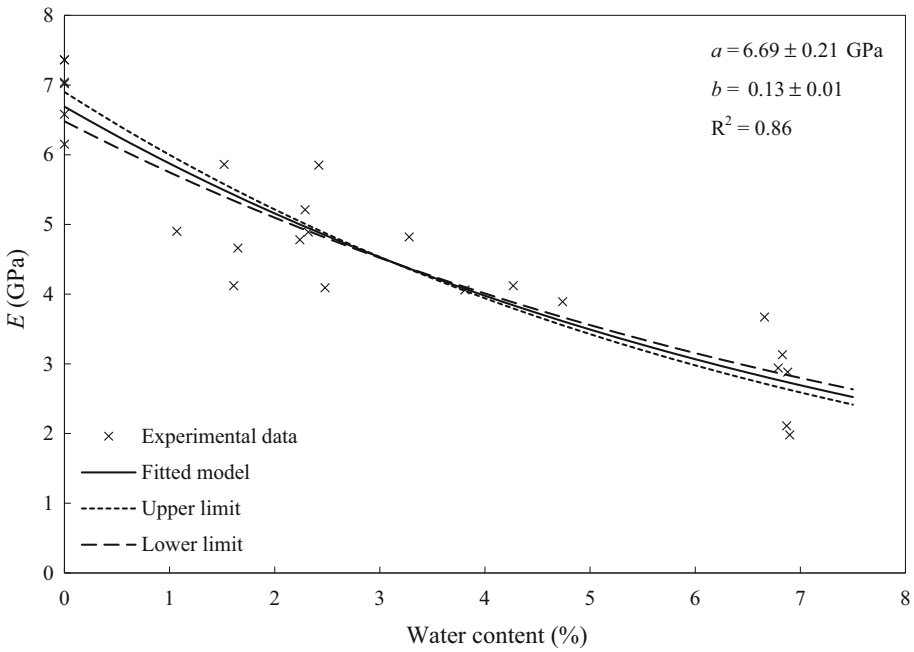

Fig. 2 Young's moduli results obtained from different water contents having Hawkins and McConnell (1992) empirical model fitted to the data along with the validity range of the fitting parameters

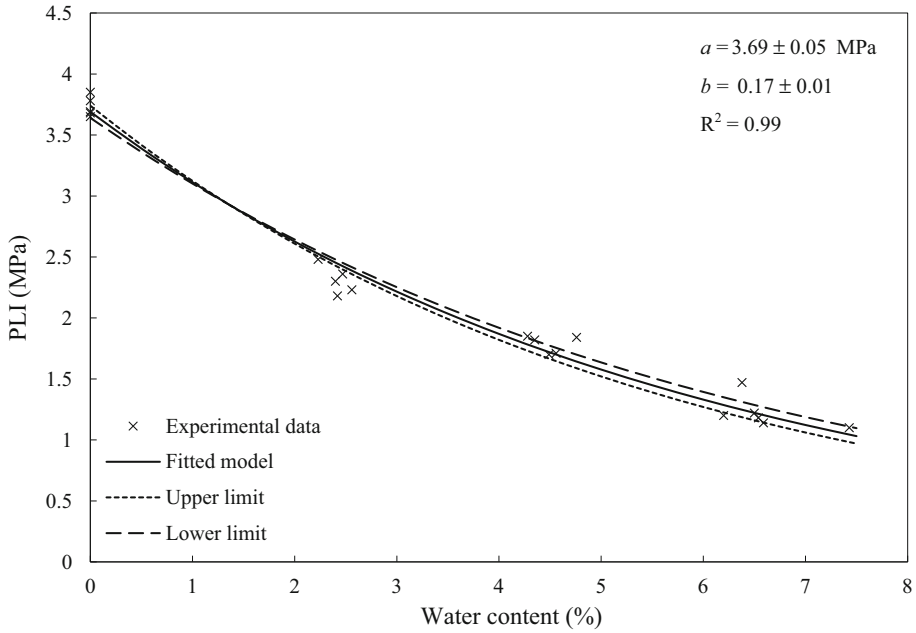

Fig. 3 Point-load index (PLI) results obtained from different water contents having Hawkins and McConnell (1992) empirical model fitted to the data along with the validity range of the fitting parameters

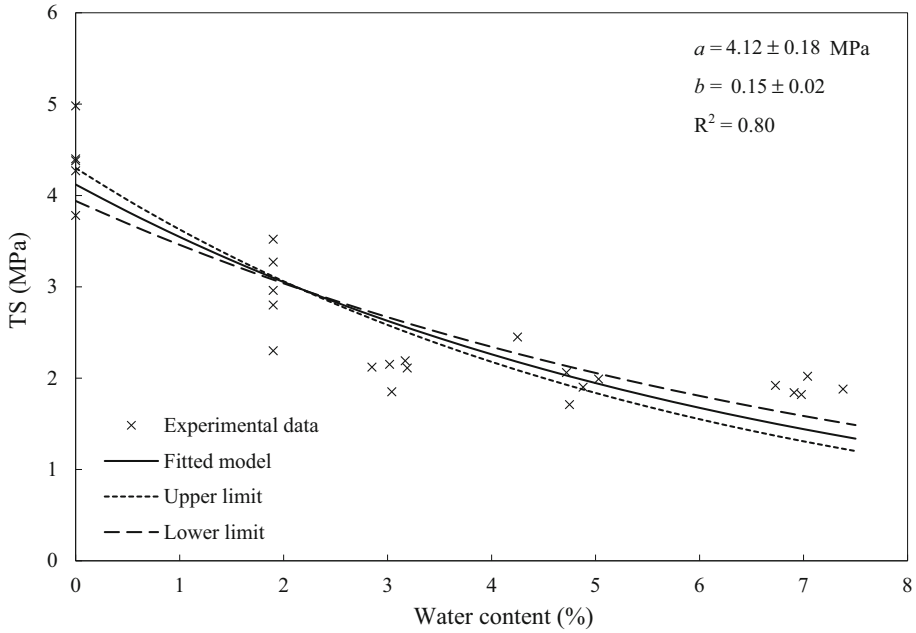

Fig. 4 Tensile strength (TS) results obtained from different water contents having Hawkins and McConnell (1992) empirical model fitted to the resulting data along with the validity range of the fitting parameters

The above analysis provides a tool with which to estimate the UCS of Gosford sandstone from a relatively simple and quick diametral point-load test. Also, it is important to note that by measuring the water content in a core sample of Gosford sandstone, a realistic estimate of the mechanical properties such as UCS, *E*, PLI and TS can be obtained from the predictive empirical models presented in this study.

4 Conclusions

This research has established a comprehensive set of empirical relationships for the effects of water content on the mechanical properties of Gosford sandstone. It was observed that all the mechanical parameters decreased with an increase in water content. The role of water content can be explained through its effects on some intrinsic strength

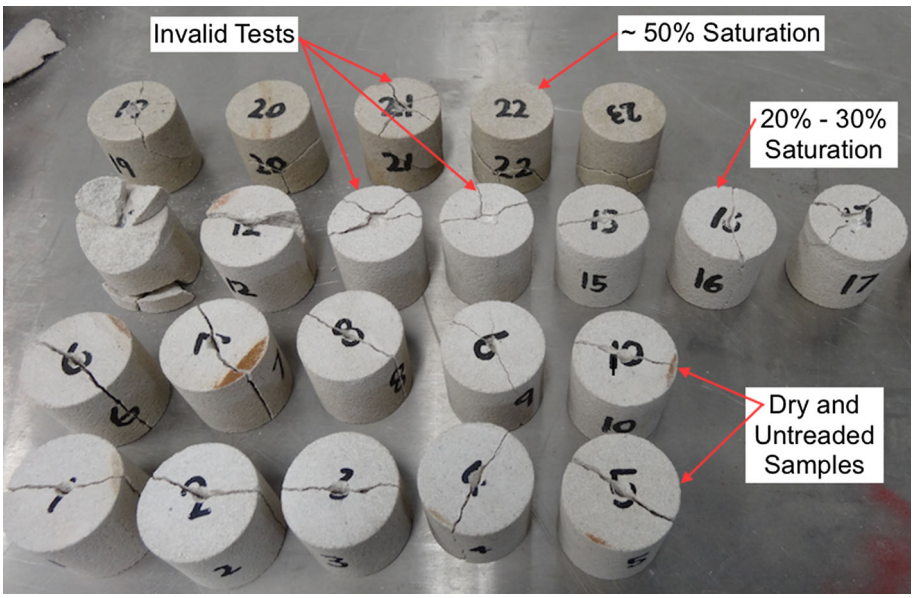

Fig. 5 Partially saturated samples tested under axial loading resulted in invalid failure patterns

parameters of rock samples such as friction coefficient, fracture toughness and initial damage which all contribute to micromechanical and macroscale failure of rock. Also, it was found that the axial point loading on the partially saturated Gosford sandstone samples leads to invalid test results.

A set of predictive empirical models were obtained for the mechanical properties of Gosford sandstone based on the original empirical model proposed by Hawkins and McConnell (1992). It was shown that there is a good agreement between the empirical model predictions and the experimental data.

References

ASTM (2010) Standard test method for measurement of hydraulic conductivity of saturated porous materials using a flexible wall permeameter. ASTM D5084. West Conshohocken, PA, United States: American Society for Testing and Materials International

Baud P, Zhu W, Wong TF (2000) Failure mode and weakening effect of water on sandstone. J Geophy R 105:16371–16389

Bieniawski ZT, Bernede MJ (1979) Suggested methods for determining the uniaxial compressive strength and deformability of rock materials: part 1. Suggested method for determining deformability of rock materials in uniaxial compression. Int J Rock Mech Min Sci 16:135–140

Bieniawski ZT, Hawkes I (1978) Suggested methods for determining tensile strength of rock materials. Int J Rock Mech Min Sci 15:99–103

Chenevert ME (1970) Shale alteration by water adsorption. J Petr Tech 22:1141–1147

Duda M, Renner J (2013) The weakening effect of water on the brittle failure strength of sandstone. Geophy J Int 92:1091–1108

Erguler Z, Ulusay R (2009) Water-induced variations in mechanical properties of clay-bearing rocks. Int J Rock Mech Min Sci 46:355–370

Fairhurst CE, Hudson JA (1999) Draft ISRM suggested method for the complete stress–strain curve for intact rock in uniaxial compression. Int J Rock Mech Min Sci 36:279–289

Fischer GJ, Paterson MS (1992) Measurement of permeability and storage capacity in rocks during deformation at high temperature and pressure. In: Evans B, Wong TF (eds) Fault mechanics and transport properties of rocks. Academic Press, San Diego, pp 213–252

Franklin JA (1985) Suggested method for determining point load strength. Int J Rock Mech Min Sci 22:51–60

Franklin JA, Vogler UW, Szlavin J, Edmund JM, Bieniawski ZT (1979) Suggested methods for determining water content, porosity, absorption and related properties. Int J Rock Mech Min Sci Geomech Abstr 16:151–156

Hadizdeh J, Law R (1991) Water-weakening of sandstone and quartzite deformed at various stress and strain rates. Int J Rock Mech Min Sci 28:431–439

Hawkins AB, McConnell BJ (1992) Sensitivity of sandstone strength and deformability to changes in moisture content. Q J Eng Geol 25:115–130

ISRM (2007) The complete suggested methods for rock characterization, testing and monitoring: 1974–2006 ISRM. In: Ulusay R, Hudson JA (eds) Suggested methods prepared by the commission on testing methods. ISRM Turkish National Group, Kozan ofset, Ankara

Kumpel HJ (1991) Poroelasticity: parameters reviewed. Geophys J Int 105:783–799

Lashkaripour GR, Passaris EKS (1995) Correlations between index parameters and mechanical properties of shales. In: 8th ISRM Congress, Tokyo, Japan, 25–29 September. International Society for Rock Mechanic, pp 257–261

Li Z, Reddish DJ (2004) The effect of groundwater recharge on broken rocks. Int J Rock Mech Min Sci 41:280–285

Lia D, Wonga LNY, Liua G, Zhanga X (2012) Influence of water content and anisotropy on the strength and deformability of low porosity meta-sedimentary rocks under triaxial compression. Eng Geol 126:46–66

Lisabeth HP, Zhu W (2015) Effect of temperature and pore fluid on the strength of porous limestone. J Geophys Res Solid Earth 120:6191–6208

Masoumi H, Douglas K, Russell AR (2016a) A bounding surface plasticity model for intact rock exhibiting size-dependent behaviour. Rock Mech Rock Eng 49:47–62

Masoumi H, Saydam S, Hagan PC (2016b) Unified size-effect law for intact rock. Int J Geomech 16:04015059

Nicolas A, Fortin J, Regnet JB, Dimanov A, Guéguen Y (2016) Brittle and semi-brittle behaviours of a carbonate rock: influence of water and temperature. Geophys J Int 206:438–456

Ojo O, Brook N (1990) The effect of moisture on some mechanical properties of rock. Min Sci Tech 10:145–156

Ord A, Vardoulakis I, Kajewski R (1991) Shear band formation in gosford sandstone. Int J Rock Mech Min Sci 28:397–409

Roshan H, Andersen MS, Acworth IR (2015) Effect of solid–fluid thermal expansion on thermo-osmotic tests: an experimental and analytical study. J Petrol Sci Eng 126:222–230

Roshan H et al (2016) Total porosity of tight rocks: a welcome to heat transfer technique. Energy Fuels 30:10072–10079

Rutter EH (1974) The influence of temperature, strain rate and interstitial water in the experimental deformation of calcite rocks. Tectonophysics 22:311–334

Sufian A, Russell AR (2013) Microstructural pore changes and energy dissipation in Gosford sandstone during pre-failure loading using X-ray CT. Int J Rock Mech Min Sci 57:119–131

Töröka A, Vásárhelyib B (2010) The influence of fabric and water content on selected rock mechanical parameters of travertine, examples from Hungary. Eng Geol 115:237–245

Vásárhelyia B (2005) Statistical analysis of the influence of water content on the strength of the Miocene limestone. Rock Mech Rock Eng 38:69–76

Vásárhelyia B, Vánb P (2006) Influence of water content on the strength of rock. Eng Geol 84:70–74

Wong LNY, Jong MC (2014) Water saturation effects on the brazilian tensile strength of gypsum and assessment of cracking processes using high-speed video. Rock Mech Rock Eng 47:1103–1115

Yao Q, Chen T, Ju M, Liang S, Liu Y, Li X (2016) Effects of water intrusion on mechanical properties of and crack propagation in coal. Rock Mech Rock Eng 49:4699–4709

Zhou Z, Cai X, Cao W, Li X, Xiong C (2016) Influence of water content on mechanical properties of rock in both saturation and drying processes. Rock Mech Rock Eng 49:3009–3025